pp 1350–1370.
doi:10.1017/aer.2020.28

Novel second-order sliding mode guidance law with an impact angle constraint that considers autopilot lag for intercepting manoeuvering targets

W.J. Zhang, **Q.L. Xia and W. Li**
bit_zhangwenjie@outlook.com
School of Aerospace Engineering
Beijing Institute of Technology
Beijing
People's Republic of China

ABSTRACT

A novel second-order sliding-mode-based impact angle and autopilot lag guidance law for engaging manoeuvering targets with unknown acceleration is presented in this study. A backstepping technique is applied to the design of the sliding surface. The proposed guidance law is based on a new sliding surface. It exhibits the advantage of ensuring that the sliding surface and its derivative will converge to zero in finite time while guaranteeing that the sliding surface will not cross zero until the ultimate time. The method effectively eliminates the undesired chattering of the sliding surface. To compensate for the uncertainty caused by target manoeuvering, a new observer is developed to estimate target manoeuvering. The convergence of the system is proven through a Lyapunov function and finite time convergence theory. Lastly, mathematical simulations results show that the proposed guidance law can achieve precise interception with a wide range of impact angles, thereby verifying the effectiveness of the guidance law.

Keywords: impact angle constraint; second-order sliding mode; autopilot lag; manoeuvering target; observer

1.0 INTRODUCTION

Guidance systems for missiles have developed rapidly in recent years, such that merely hitting the target accurately has become insufficient, but an expected impact angle is also required

Received 17 May 2019; revised 2 February 2020; accepted 11 March 2020.

for missiles. A specific impact angle may increase the power of a warhead, which motivates the development of a guidance law with impact angle constraints.

To date, considerable research concerned with impact angle constraint problems has been conducted. Literature[1] studied impact angle problems and derived a suboptimal guidance law through optimal control theory. Literature[2] provided an optimal solution for an ordinary intersection problem by minimising the performance index for terminal position and velocity constraints. This solution could be used for impact angle constraint problems if the intersection procedure was defined as an expected collision process. The performance index was selected as an apposite time-varying weighting function in Literature[3] for an optimal impact angle constraint guidance law. A traditional guidance law to achieve the expected impact angle was obtained by adjusting the gain of the weighting functions. In Literature[4], arbitrary order missile dynamics were considered in optimal impact angle constraint problems, thereby providing a generalised formulation. In Literature[5], the state-dependent Riccati equation method, which was widely used in various types of nonlinear control issues, was applied to cope with impact angle constraint problems. In Literature[6], a linear time-varying guidance law was addressed using the inverse problem in optimal control theory to obtain the expected impact angle and minimal miss distance. With the progress of model predictive static programming and generalised model predictive static programming approaches in recent years, Literature[7] and [8] proposed new suboptimal guidance commands to accomplish specific impact angles.

As indicated above, considerable researches have been performed based on optimal control theory. However, proportional navigation (PN) guidance laws are more widely used to solve impact angle constraint problems. In Literature[9], a time-varying bias term was added to the traditional PN, called the biased PN guidance law, and the bias term achieved impact angle constraints. In Literature[10–12], a two-phase guidance approaches for controlling the impact angle were proposed. In Literature[10], the guidance law consisted of a PN coefficient with two phases: one for generating an orientation trajectory to cover all impact angles from 0 to $-\Pi$ with navigation gain $N < 2$ and the other for attacking a stationary target at a desired impact angle with $N \geq 2$. In Literature[11], the approach was further developed for the case of nonstationary nonmanoeuvering targets. In Literature[12], another two-phase guidance approach that consisted of a conventional PN term and a biased PN term was proposed. The desired impact angle was satisfied by adjusting the integral of the bias term.

Variable structure control theory has been gradually applied to guidance law systems in recent years due to its robustness and simple control algorithm[13,14]. The sliding mode can be designed as necessary and is independent of object parameters and disturbances. Thus, the terminal condition can be incorporated into the sliding mode to obtain the guidance law, thereby satisfying terminal constraints. The core of this type of guidance is determining how to select the switching function of the sliding surface to meet the requirements for zeroing in missed distance and impact angle constraints and to ensure that the system reaches the sliding surface in finite time. In Literature[15], a new guidance law was established using a high-performance sliding mode technique, which not only satisfied the terminal angle constraint but also enhanced the observabilities of stationary and slow-moving targets. Literature[16] proposed a linear sliding mode guidance law (LSMGL) to intercept nonmanoeuvering targets in an expected impact angle. In Literature[17], a terminal sliding mode (TSM) based on robust control was presented to intercept stationary or slow-moving targets whose terminal constraints were the impact angle and the seeker's field-of-view limit. In Literature[18] and [19], TSM and nonsingular TSM (NTSM) guidance laws were developed for manoeuvering targets, respectively, and preset angle limits were implemented. However, the two studies

https://doi.org/10.1017/aer.2020.28 Published online by Cambridge University Press

have shortcomings: (1) the control input chattering problem and (2) the upper bound acceleration of the target manoeuvering was required. The target information is usually difficult to obtain in advance for practical applications. Therefore, a large value of switching gain is consumed to ensure the stability of sliding variable structure control, which increases the amount of control energy. Literature[20] provided a precise interception guidance law that considered impact angle constraints without the information of the target and used a disturbance observer to estimate target information in real time, thereby solving the aforementioned problems. In practical applications, a precision guidance system will be influenced by autopilot lag, particularly if target manoeuvering exists, thus autopilot delay in a guidance system design process should be considered[21].

In the past decade, backstepping design procedures have been intensively introduced[22–25]. The backstepping control is a systematic and recursive design method for nonlinear systems to offer a choice to accommodate the unmodeled nonlinear effects and parameter uncertainties. The essence of backstepping design is to select some appropriate functions of state variables as pseudocontrol inputs for lower dimension subsystems of the overall system. Each backstepping stage results in a new pseudocontrol design, expressed in terms of the pseudocontrol designs from preceding design stages. When the procedure is terminated, a feedback design for the true control input results, which achieves the original design objective by virtue of a final Lyapunov function, which is formed by summing up the Lyapunov functions associated with each individual design stage[26]. In[27], the author developed a backstepping design method of tracking controller for the systems under consideration. In[28], based on the observer methodology, the adaptive fuzzy backstepping technique was extended to uncertain multiple-input and multiple-output (MIMO) systems, and an adaptive controller was developed. Then, for nonlinear time-delay systems, backstepping-based controllers were designed in[29].

The essence of guidance system is a nonlinear control problem, and usually the dynamics of the system is completely matched with its mathematical model. There are, of course, unavoidable model uncertainties for any practical system including the guidance systems, which lead the degradation of controller performance. For the guidance system, the target manoeuvering is an uncertainty, if the manoeuvering is not considered in the control command, the guidance performance will be reduced. In these cases, the conventional control approaches are not applicable, and usually the universal functions approximators (UFAs)-based adaptive approaches are suggested to address this issue[30]. Therefore, the analytical study of adaptive control of uncertain nonlinear systems using UFA has received much attention during last decade[31]. In this regards, neural networks (NNs) and fuzzy logic (FL) are usually exploited to approximate the unknown uncertainties[32]. Then, adaptive laws are designed to adjust the parameters of the NNS and FL. Another important method to deal with these problems is to use the observer[17], which is the method adopted in this paper.

Motivated by these situations, the present study proposes a novel second-order sliding-mode guidance law (NSO-SMGL) using backstepping technique by considering autopilot lag. For target manoeuvering, this study adopts a general disturbance observer to estimate the manoeuvering and compensate for it in the guidance law. Through the designed command, the missile achieves precise interception with the desired impact angle even if autopilot delay exists. The convergence of the guidance system is proven through Lyapunov stability theorem, which ensures that the sliding surface and its derivative will converge to zero in finite time and guarantees that the sliding surface will not cross zero as what happened in[33], thereby effectively eliminating undesired chattering.

https://doi.org/10.1017/aer.2020.28 Published online by Cambridge University Press

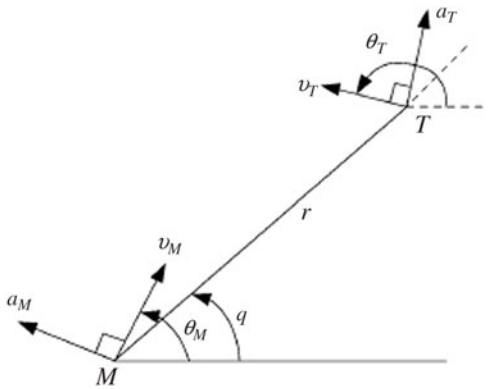

Figure 1. Relative motion between the missile and the target.

The remainder of this paper is organised as follows. Section 2 establishes the kinematics equations between a missile and a target. Several theoretical bases are also given. Section 3 introduces the general disturbance observer and the approach to apply NSO-SMGL. The convergence of the sliding control method is also proven. Section 4 provides the expression for the proposed NSO-SMGL. Section 5 presents the simulation results of the derived guidance law for several typical situations. Section 6 gives the conclusions of the study.

2.0 PRELIMINARY

In this section, missile interception engagement on a vertical plane, including impact angle definition and an autopilot model, are derived. Necessary fundamental theories are also presented.

2.1 Problem formulation

The geometric relationship between the relative motion of a missile and a target on a vertical plane is established in Fig. 1. In the figure, M and T denote the positions of the missile and the target, respectively. v_M and v_T indicate the velocity of the missile and the target, respectively. a_M and a_T represent the normal acceleration of the missile and the target, respectively. θ_M and θ_T are the flight path angle of the missile and the target, respectively. q is the line-of-sight (LOS) angle between the missile and the target. r is the relative distance between the missile and the target. The relative motion equation between the missile and the target can be obtained from Fig. 1

$$\dot{r} = v_T \cos(q - \theta_T) - v_M \cos(q - \theta_M), \quad \ldots (1)$$

$$r\dot{q} = -v_T \sin(q - \theta_T) + v_M \sin(q - \theta_M), \quad \ldots (2)$$

$$\dot{\theta}_M = a_M / v_M, \quad \ldots (3)$$

$$\dot{\theta}_T = a_T / v_T, \quad \ldots (4)$$

https://doi.org/10.1017/aer.2020.28 Published online by Cambridge University Press

where $\dot{r}$ is the derivative of the relative distance with respect to time, $\dot{q}$ is the derivative of the LOS angle q, it represents the LOS angular rate, and $\dot{\theta}_M$ and $\dot{\theta}_T$ are the derivatives of the missile's and target's flight path angles with respect to time.

When both sides of Equation (2) are differentiated with respect to time, the following equation can be derived:

$$\ddot{q} = -2\frac{\dot{r}}{r}\dot{q} + \frac{\dot{v}_M \sin(q-\theta_M) - a_M \cos(q-\theta_M)}{r} + \frac{a_T \cos(q-\theta_T) - \dot{v}_T \sin(q-\theta_T)}{r}, \quad \ldots(5)$$

where $\dot{v}_M$ and $\dot{v}_T$ are the tangential accelerations of the missile and the target; and $\ddot{q}$ is the derivative of the LOS angular rate with respect to time.

For the convenience of derivation, we firstly assume that the missile and the target are flying in a constant tangential speed. In fact, the guidance law is suitable for a varying speed missile because the tangential velocity is treated as the system uncertainty and is estimated and compensated by the observer together with the target manoeuvering. Then, Equation (5) can be organised as

$$\ddot{q} = -2\frac{\dot{r}}{r}\dot{q} - \frac{a_{Mq}}{r} + \frac{a_{Tq}}{r}, \quad \ldots(6)$$

where $a_{Mq} = a_M \cos(q-\theta_M)$ and $a_{Tq} = a_T \cos(q-\theta_T)$ are the components of the missile and the target accelerations that are perpendicular to the LOS, respectively.

In accordance with the principle of parallel approach, the purpose of a guidance law is to make the LOS angular rate $\dot{q}$ approach to zero by adjusting a_{Mq}, thereby ensuring that the missile will attack the target accurately.

Assumption 1. Given the missile's and the seeker's physical limits, the missile's and the target's acceleration components and their first and second derivatives (a_{Mq}, a_{Tq}, $\dot{a}_{Tq}$, and $\ddot{a}_{Tq}$) are bounded by the following conditions:

$$|a_{Mq}| \le A_m,\ |a_{Tq}| \le A_t,\ |\dot{a}_{Tq}| \le A_1,\ |\ddot{a}_{Tq}| \le A_2; \quad \ldots(7)$$

where A_m, A_t, A_1, and A_2 are unknown bounds which represent the manoeuverability; and the seeker's minimum working distance is r_0. The variable r satisfies

$$r \ge r_0, \quad \ldots(8)$$

Considering the dynamic model of the autopilot, the autopilot model is approximated to the first-order inertia as follows:

$$\dot{a}_{Mq} = -\frac{1}{\tau}a_{Mq} + \frac{1}{\tau}u, \quad \ldots(9)$$

where τ is the autopilot dynamic lag constant of the missile, and u is the guidance command acceleration to be provided to the missile.

For problems with an impact angle constraint, the impact angle is first defined as the angle between the velocity vector of the missile and the target at the end of the collision. Therefore, considering the constraint on the impact angle, the flight path angle should be strictly limited

https://doi.org/10.1017/aer.2020.28 Published online by Cambridge University Press

when the missile is hitting the target. Defining the end of guidance as t_f, the expected impact angle of the missile is θ_d, and the desired LOS angle is q_d at the end of guidance. Therefore, the design of the guidance law that considers the impact angle constraint refers to the missile hitting the target accurately at the desired impact angle; that is[33],

$$\lim_{t\to t_f} r(t)\,\dot{q}(t) \to 0, \quad \ldots(10)$$

$$\theta_M\left(t_f\right) - \theta_T\left(t_f\right) = \theta_d, \quad \ldots(11)$$

$$\left|\theta_M\left(t_f\right) - q_d\right| < \frac{\pi}{2}. \quad \ldots(12)$$

Equation (12) indicates that the target is within the field of view of the missile's seeker when the missile hits the target. From Equations (2) and (10):

$$v_T \sin\left(\theta_T\left(t_f\right) - q_d\right) \approx v_M \sin\left(\theta_M\left(t_f\right) - q_d\right). \quad \ldots(13)$$

From Equation (13), a unique flight path angle of the missile $\theta_M\left(t_f\right)$ can be ascertained if the flight path angle of target $\theta_T\left(t_f\right)$ is known for the desired missile impact angle θ_d. Then, the desired LOS angle can be obtained from Equations (10) and (12). Hence, the control of the impact angle can be transformed into the control of the final LOS angle.

2.2 Fundamental theories

Before designing the guidance law, the definition of finite-time stability in sliding mode control is first introduced.

Definition 1[34]. Consider the following system:

$$\dot{x}(t) = f(x,t), x \in \mathbf{R}^n, \quad \ldots(14)$$

where $f(x): D \to \mathbf{R}^n$ is defined as a value of D in n dimensional space $\mathbf{R}^n$ that satisfies the local Lipschitz continuous condition. For the system Equation (14), $f(x): U \to \mathbf{R}^n$ is a continuous function for x on the semi-open domain U containing the origin. Finite-time convergence is represented by $\forall x_0 \in U_0 \subset \mathbf{R}^n$, there exists a continuous function $T(x): U_0 \setminus \{0\} \to (0, +\infty)$, thereby making the solution of the system Equation (14) $x(x_0, t)$ satisfy: when $t \in [0, T(x_0)]$, there exists $x(x_0, t) \in U_0 \setminus \{0\}$ and $\lim_{t\to T(x_0)} x(x_0, t) = 0$, and when $t > T(x_0)$, there exists $x(x_0, t) = 0$. Suppose the equilibrium point of the system Equation (14) is $x = 0$, when and only when the system is strongly stable and converges in a limited time, the equilibrium point $x = 0$ of the system is then regarded as stable in a finite time. If $U = U_0 \in \mathbf{R}^n$, then the equilibrium point is stable globally in a finite time.

Lemma 1[35]. *Suppose the existence of a continuous differentiable positive definite function $V(x)$ defined in a neighborhood of the origin. For the real numbers $c > 0$ and $0 < \beta < 1$, there is $\dot{V}(x) + cV^{\beta}(x) \le 0$ and $x \in U \setminus \{0\}$. Then, the system could converge to origin in finite time, and the upper bound of the convergence time is satisfied as follows:*

$$T(x_0) \le \frac{V^{1-\beta}(x_0)}{c(1-\beta)}. \quad \ldots(15)$$

https://doi.org/10.1017/aer.2020.28 Published online by Cambridge University Press

3.0 TARGET MANOEUVERING ESTIMATOR AND SECOND-ORDER SLIDING MODE THEORY

An estimation of target manoeuvering is required to effectively intercept manoeuvering targets. A general disturbance observer is presented in the first part of this section, and then a novel second-order sliding mode theory is established in the next part.

3.1 Target manoeuvering estimator

Consider the following system:

$$\dot{x} = f + bu + d. \qquad \ldots(16)$$

where f is the known state variable of the system; u and b are the control input and coefficient, respectively; and d represents target manoeuvering, which is regarded as system interference.

For System Equation (15), the general disturbance observer is defined as

$$\begin{cases} \dot{z}_0 = z_1 + k_1 |x - z_0|^{1-1/p} \mathrm{sgn}\,(x - z_0) + f + bu \\ \dot{z}_1 = k_2 |x - z_0|^{1-2/p} \mathrm{sgn}\,(x - z_0) \end{cases}, \qquad \ldots(17)$$

where $k_1, k_2 > 0$ and $p > 2$ are parameters to be designed; and z_0 and z_1 are estimations of x and d, respectively.

Theorem 1[36]. *Variables $\eta_1 = x - z_0$ and $\eta_2 = d - z_1$ are defined as estimation errors. If the derivative of system interference satisfies $|\dot{d}| \le \dot{d}^{\max}$ with $\dot{d}^{\max}$ being a positive constant, then the vector can converge to the following domain in finite time:*

$$\|\eta\| \le \left(\frac{\dot{d}^{\max} \|\boldsymbol{B}\|}{\lambda_{\min}(\boldsymbol{Q})} \right)^{(p-1)/(p-2)}, \qquad \ldots(18)$$

where $\boldsymbol{\eta} = [\eta_1, \eta_2]^T$, $\lambda_{\min}(\cdot)$ refers to the minimum eigenvalue of matrix $(\cdot)$ and the vector 2-norm $\|\cdot\|$, and

$$\boldsymbol{Q} = \begin{bmatrix} k_1 k_2 + k_1^3 \frac{p-1}{p} & -k_1^2 \frac{p-1}{p} \\ -k_1^2 \frac{p-1}{p} & k \frac{p-1}{p} \end{bmatrix}, \boldsymbol{B} = \begin{bmatrix} -k_1 \\ 2 \end{bmatrix}, \qquad \ldots(19)$$

Proof of Theorem 1. According to Equations (16) and (17), the estimation error variable can be acquired as

$$\begin{cases} \dot{\eta}_1 = \eta_2 - k_1 |\eta_1|^{1-1/p} \mathrm{sgn}\,(\eta_1) \\ \dot{\eta}_2 = \dot{a}_{Tq} - k_2 |\eta_1|^{1-2/p} \mathrm{sgn}\,(\eta_1) \end{cases}, \qquad \ldots(20)$$

For differential Equation (16), construct the Lyapunov function as follows

$$V_1 = \frac{k_2 p}{p-1} |\eta_1|^{2(p-1)/p} + \frac{1}{2}\eta_2^2 + \frac{1}{2}\left(k_1 |\eta_1|^{(p-1)/p} \mathrm{sgn}\,(\eta_1) - \eta_2\right)^2, \qquad \ldots(21)$$

https://doi.org/10.1017/aer.2020.28 Published online by Cambridge University Press

which can be written as the following vector form

$$V_1 = \boldsymbol{\eta}^T \boldsymbol{P} \boldsymbol{\eta}, \qquad \ldots (22)$$

where

$$\boldsymbol{P} = \frac{1}{2}\begin{bmatrix} \frac{k_2 p}{p-1} + k_1^2 & -k_1 \\ -k_1 & 2 \end{bmatrix}, \qquad \ldots (23)$$

As $k_2 > 0$ and $p > 2$ are positive definite and radially unbounded, that is

$$\lambda_{\min}(\boldsymbol{P}) \|\boldsymbol{\eta}\|^2 \le V_1 \le \lambda_{\max}(\boldsymbol{P}) \|\boldsymbol{\eta}\|^2, \qquad \ldots (24)$$

where $\lambda_{\max}(\cdot)$ refers to the maximum eigenvalue of matrix $(\cdot)$.

Advert that V_1 is continuously differentiable, except on the set $\Omega = \{(\eta_1, \eta_2) \in R^2 \,|\, \eta_1 = 0\}$. However, if $\eta_1 = 0$, $\eta_2 \neq 0$, one can imply $\dot{\eta}_1 = \eta_2 \neq 0$, this means that the trajectories of system Equation (20) just cross the area Ω and cannot maintain on it, except when the initial values $\eta_1 = 0$, $\eta_2 = 0$, have been achieved. Thus, the time derivative of V_1 can be calculated by derivation as

$$\begin{aligned} \dot{V}_1 = & \left(\frac{k_2 p}{p-1} + \frac{1}{2}k_1^2\right)\frac{2p-2}{p}|\eta_1|^{(p-2)/p}\mathrm{sgn}(\eta_1) \\ & \left(\eta_2 - k_1|\eta_1|^{(p-1)/p}\mathrm{sgn}(\eta_1)\right) \\ & + \left(2\eta_2 - k_1|\eta_1|^{(p-1)/p}\mathrm{sgn}(\eta_1)\right)\left(\dot{a}_{Tq} - k_2|\eta_1|^{(p-2)/p}\mathrm{sgn}(\eta_1)\right) \\ & - k_1\frac{p-1}{p}|\eta_1|^{-1/p}\left(\eta_2 - k_1|\eta_1|^{(p-1)/p}\mathrm{sgn}(\eta_1)\right), \\ = & -|\eta_1|^{-1/p}\left(k_1 k_2|\eta_1|^{2(p-1)/p} + \frac{p-1}{p}k_1^3|\eta_1|^{2(p-1)/p}\right. \\ & \left. -2\frac{p-1}{p}k_1^2|\eta_1|^{(p-1)/p}\mathrm{sgn}(\eta_1)\,\eta_2 + \frac{p-1}{p}k_1\eta_2^2\right) \\ & + \left(2\eta_2 - k_1|\eta_1|^{(p-1)/p}\mathrm{sgn}(\eta_1)\right)\dot{a}_{Tq} \\ \le & -|\eta_1|^{-1/p}\boldsymbol{\eta}^T\boldsymbol{P}\boldsymbol{\eta} + \dot{d}^{\max}(x)\,\boldsymbol{B}\boldsymbol{\eta} \end{aligned} \qquad \ldots (25)$$

As $k_1, k_2 > 0$ an $p > 2$, obviously, the matrix $\boldsymbol{Q}$ is Hurwitz. Moreover, from the fact that $\|\boldsymbol{\eta}\| = \sqrt{|\eta|^{2(p-1)/p} + \eta_2^2} \ge |\eta_1|^{(p-1)/p}$, one can imply $|\eta_1|^{-1/p} \ge \|\boldsymbol{\eta}\|^{-1/(p-1)}$. Then, from Equations (24) and (25) one can get

$$\begin{aligned} \dot{V}_1 & \le -|\eta_1|^{-1/p}\lambda_{min}(\boldsymbol{Q})\|\boldsymbol{\eta}\|^2 + \dot{d}^{\max}(x)\|\boldsymbol{B}\|\|\boldsymbol{\eta}\| \\ & \le -\left(\lambda_{min}(\boldsymbol{Q})\|\boldsymbol{\eta}\|^{(p-2)/(p-1)} - \dot{d}^{\max}(x)\|\boldsymbol{B}\|\right)\|\boldsymbol{\eta}\|, \\ & \le -\left(\lambda_{min}(\boldsymbol{Q})\|\boldsymbol{\eta}\|^{(p-2)/(p-1)} - \dot{d}^{\max}(x)\|\boldsymbol{B}\|\right)\frac{V_1^{1/2}}{\sqrt{\lambda_{\max}(\boldsymbol{P})}} \end{aligned} \qquad \ldots (26)$$

https://doi.org/10.1017/aer.2020.28 Published online by Cambridge University Press

If $\lambda_{min}(\boldsymbol{Q})\|\boldsymbol{\eta}\|^{(p-2)/(p-1)} - \dot{d}^{\max}(x)\|\boldsymbol{B}\| > 0$, Equation (26) can be written as

$$\dot{V}_1 \leq -\frac{\gamma V_1^{1/2}}{\sqrt{\lambda_{\max}(\boldsymbol{P})}}, \quad \ldots(27)$$

where $\gamma = \lambda_{min}(\boldsymbol{Q})\|\boldsymbol{\eta}\|^{(p-2)/(p-1)} - \dot{d}^{\max}(x)\|\boldsymbol{B}\| > 0$, In the light of Lemma 1, the area

$$\|\eta\| \leq \left(\frac{\dot{d}^{\max}(x)\|\boldsymbol{B}\|}{\lambda_{\min}(\boldsymbol{Q})}\right)^{(p-1)/(p-2)}, \quad \ldots(28)$$

can be approached in finite time, which also proves that the estimation errors will be converge in a small area around zero in finite time. The proof is completed.

Remark 1. By proper parameter selection, $\left|\dot{d}^{\max}\|\boldsymbol{B}\|/\lambda_{\min}(\boldsymbol{Q})\right| < 1$ can be obtained. Furthermore, as $p > 2$, a sufficiently large value of $(p-1)/(p-2)$ can be achieved. Therefore, the value of $\left(\dot{d}^{\max}\|\boldsymbol{B}\|/\lambda_{\min}(\boldsymbol{Q})\right)^{(p-1)/(p-2)}$ can be tuned very close to zero and highly precise estimation performance can be assured.

Remark 2. It should be noted that the setting of p is very important. If one set $p = 2$, the presented target manoeuvering estimator reduces to classical super-twisting observer. However, the term $|x - z_0|^{1-2/p}\mathrm{sgn}(x - z_0)$ in Equation (17) with $p = 2$ is discontinuous while the proposed estimator is continuous and therefore the undesired chattering can be mitigated significantly.

Remark 3. Compared with classical linear state observer, the proposed observer has two main advantages: (1) guarantee finite-time convergence of the target manoeuvering estimation error; (2) exhibits strong robustness against the variation of target manoeuverings.

3.2 Second-order sliding mode control

In general, we use the first-order sliding mode method to deal with problems with a relative degree of 1[37]. However, a higher-order sliding mode method should be used for problems with larger degrees. In higher-order sliding mode, the sliding surface and its successive derivatives will converge to zero; that is,

$$s, \dot{s}, \ddot{s}, \ldots s^{\kappa} = 0, \quad \ldots(29)$$

where κ is the relative degree. The second-order sliding mode method is widely adopted in guidance system design. This method can be used to deal with problems with a relative degree of 2 or to eliminate chattering with a relative degree of 1. One example of an extensive second-order sliding mode method is the super-twisting algorithm[15], in which the sliding surface and its derivative make countless twists around the origin and converge to zero in finite time. Despite being a useful method that has been considerably studied, the super-twisting algorithm exhibits a drawback, i.e., the sliding surface is forced to oscillate near the equilibrium point (zero), which results in command chattering. NSO-SMGL, which is based on a backstepping technique, is deduced in this section. This approach exhibits the advantage

https://doi.org/10.1017/aer.2020.28 Published online by Cambridge University Press

of ensuring that the sliding surface and its derivative converge to zero in finite time while guaranteeing that the sliding surface will not cross zero until the ultimate time.

First, the desired sliding surface is defined as follows:

$$s = f = 0. \quad \ldots (30)$$

The first and second derivatives of the sliding surface Equations (30) are

$$\dot{s} = h, \quad \ldots (31)$$

$$\ddot{s} = f + bu + d, \quad \ldots (32)$$

where h, f, and b are known functions of the system; and d represents target manoeuvering, which is assumed as a bounded uncertainty. The guidance command u emerges in the second derivative of the sliding surface; thus, surface Equations (30) has a relative degree of 2.

The objective is to search for a formula for sliding surface Equations (30) and its derivative Equations (31). Both equations converge to zero at an expected time t_r. A backstepping technique is used to achieve the objective. We set $\dot{s}$ as a virtual command, and $\dot{s}$ should be designed to send s to zero. The Lyapunov function V_2 is selected.

$$V_2 = \frac{1}{2}s^2 \quad \ldots (33)$$

Considering the derivative of Equation (33) with respect to time yields

$$\dot{V}_2 = s\dot{s}. \quad \ldots (34)$$

To ensure that sliding surface Equations (30) will converge to zero in finite time, $\dot{V}_2$ must be negative infinity. Then, $\dot{s}$ can be set as

$$\dot{s} = -\frac{ns}{t_r - t}, n > 1, \quad \ldots (35)$$

where t_r is the expected convergence time. Substituting Equations (35) into Equations (34) yields

$$\dot{V}_2 = -\frac{ns^2}{t_r - t}. \quad \ldots (36)$$

Substituting Equation (33) into Equation (36) derives

$$\dot{V}_2 = -\frac{2nV_2}{t_r - t}. \quad \ldots (37)$$

Integrating Equation (37) from the initial value $(V_2(t_0), t_0)$ into the current value $(V_2(t), t)$ can result in

$$V_2(t) = \frac{V_2(t_0)}{(t_r - t_0)^{2n}}(t_r - t)^{2n}. \quad \ldots (38)$$

https://doi.org/10.1017/aer.2020.28 Published online by Cambridge University Press

Notably, when n is greater than 0.5, $(t_r - t)^{2n}$ in Equation (38) will converge to zero because t is close to t_r. Therefore, the Lyapunov function (and consequently, the sliding surface) is guaranteed to converge to zero at the expected time t_r provided that $n > 0.5$. Equation (35) depends on the values of the sliding surface and time t; it can also ensure that $\dot{s}$ converges to zero at t_r, as proven in[19]. Furthermore, achieving such goal for $\dot{s}$ places an additional constraint on parameter n, which should be satisfied as $n > 1$.

Equation (35) provides an expected trajectory for $\dot{s}$ to follow. Notably, condition Equation (35) should not necessarily be satisfied at the initial time because the initial value of $\dot{s}$ completely depends on the initial conditions of the problem. Therefore, guidance command u must be used to send $\dot{s}$ from its initial value to the trajectory defined by Equation (35) in finite time, and then $\dot{s}$ must be maintained on the trajectory. Given that the system must comply with certain actions along trajectory Equation (35) to ensure that s and $\dot{s}$ converge to zero, the trajectory should be reached in finite time.

To ensure that trajectory Equation (35) will be reached in finite time, the new sliding surface should be considered as follows:

$$s_2 = \dot{s} + \frac{ns}{t_r - t} = 0. \quad \ldots (39)$$

The time derivative of surface Equation (39) results in

$$\dot{s}_2 = f + d + \frac{n\dot{s}\,(t_r - t) + ns}{(t_r - t)^2} + bu. \quad \ldots (40)$$

As indicated in Equation (40), the new sliding surface Equation (39) has a relative degree of 1 to guidance command u.

The expression for u must be obtained to make s_2 converge to zero in finite time t_r^*. The Lyapunov function is selected as follows:

$$V_2 = \frac{1}{2} s_2^2. \quad \ldots (41)$$

The time derivative of Equation (41) yields

$$\dot{V}_2 = s_2 \dot{s}_2 = s_2 \left[f + \frac{n\dot{s}\,(t_r - t) + ns}{(t_r - t)^2} + d + bu \right] \quad \ldots (42)$$

To ensure that the Lyapunov function will converge to zero in finite time, u is exhibited as

$$u = -\frac{1}{b} \left(f + \frac{n\dot{s}\,(t_r - t) + ns}{(t_r - t)^2} + \hat{d} + \eta \operatorname{sgn}\left(\dot{s} + \frac{ns}{t_r - t} \right) \right). \quad \ldots (43)$$

where η is an appropriately positive constant, and $n > 2$. $\hat{d}$ is the estimation of target manoeuvering. If $\hat{d} \to d$ is in finite time, then $\dot{V}_2$ is a negative definite function with guidance command Equation (43), which satisfies the following inequality :

$$\dot{V}_2 < -\eta\, |s_2|, \quad \ldots (44)$$

https://doi.org/10.1017/aer.2020.28 Published online by Cambridge University Press

where η is the design parameter that satisfies $\eta > 0$ and influences the convergence speed of the system.

The consequence from the preceding derivations can be summarised in Theorem 2.

Theorem 2[38]. *Assume that a sliding surface $s = f$ has a relative degree of 2, with a second differential form $\ddot{s} = f + bu + d$. Then, with the guidance command Equation (43), s and $\dot{s}$ can converge to zero in finite time t_r.*

Remark 4. For the guidance command Equation (43), if there exists noises, the estimator can estimate the target's acceleration together with the noises, and compensate in the guidance law, which could counteract the effects of noises. Therefore, the guidance law has certain robustness when there exists noises.

In terms of the application of guidance command Equation (43), the sign function is under guidance command. To eliminate the overload command chattering problem brought by the sign function, we use the following continuous saturation function to smooth it:

$$sat\,(S,\phi) = \begin{cases} S/\phi, & |S| \le \phi \\ \mathrm{sgn}\,(S)\ , & |S| > \phi \end{cases}, \qquad \ldots (45)$$

where ϕ is the defibrillation factor, and $\phi = 0.01$ is used in the simulation.

4.0 GUIDANCE LAW DESIGN

In this section, the proposed NSO-SMGL that considers autopilot lag and impact angle constraint is developed on the basis of sliding mode theory and the target observer technique. A backstepping method is adopted to design the guidance law.

First, state variables are defined as follows:

$$x_1 = q - q_d,\ x_2 = \dot{q},\ \text{and}\, x_3 = \ddot{q}, \qquad \ldots (46)$$

where q_d is the expected LOS angle. Differentiating Equation (46) with respect to time yields the following system equations with autopilot lag and impact angle constraint:

$$\dot{x}_1 = x_2, \qquad \ldots (47)$$

$$\dot{x}_2 = -\frac{2\dot{r}}{r}x_2 - \frac{1}{r}a_{Mq} + \frac{1}{r}a_{Tq}, \qquad \ldots (48)$$

$$\dot{x}_3 = \left(-\frac{2\ddot{r}}{r} + \frac{2\dot{r}^2}{r^2}\right)x_2 - \frac{2\dot{r}}{r}x_3 + \left(\frac{\dot{r}}{r^2} + \frac{1}{r\tau}\right)a_{Mq} - \frac{1}{r\tau}u - \frac{\dot{r}}{r^2}a_{Tq} + \frac{1}{r}\dot{a}_{Tq}. \qquad \ldots (49)$$

Equation (50) is derived from Equation (48) as follows:

$$\frac{1}{r}a_{Tq} = \frac{2\dot{r}}{r}x_2 + \frac{1}{r}a_{Mq} + \dot{x}_2. \qquad \ldots (50)$$

https://doi.org/10.1017/aer.2020.28 Published online by Cambridge University Press

Substituting Equation (50) into Equation (49) yields

$$\dot{x}_3 = -\frac{2\dot{r}}{r}x_2 - \frac{3\dot{r}}{r}x_3 + \frac{1}{r\tau}a_{Mq} - \frac{1}{r\tau}u + \frac{1}{r}\dot{a}_{Tq} \quad \ldots(51)$$

Let $f_0\left(x_3, a_{Mq}\right) = -\frac{3\dot{r}}{r}x_3 + \frac{1}{r\tau}a_{Mq}$ be recorded as f_0, and $f_1\left(x_2, \dot{a}_{Tq}\right) = -\frac{2\dot{r}}{r}x_2 + \frac{1}{r}\dot{a}_{Tq}$ be recorded as f_1; $b = -\frac{1}{r\tau}$.

Then, the preceding system can be organised as

$$\begin{cases} \dot{x}_1 = x_2 \\ \dot{x}_2 = x_3 \\ \dot{x}_3 = f_0 + f_1 + bu \end{cases}. \quad \ldots(52)$$

Then, the sliding surface is defined as

$$s = m_1 x_1 + x_2. \quad \ldots(53)$$

Therefore, the first and second order derivatives of Equation (52) are

$$\dot{s} = m_1 x_2 + x_3, \quad \ldots(54)$$

$$\ddot{s} = m_1 x_3 + \dot{x}_3. \quad \ldots(55)$$

Another sliding surface that contains the message of the first sliding surface is defined as follows:

$$s_2 = \dot{s} + \frac{ns}{t_r - t}. \quad \ldots(56)$$

Differentiating Equation (55) from Equation (34) with respect to time yields

$$\begin{aligned} \dot{s}_2 &= \ddot{s} + \frac{n\dot{s}\left(t_r - t\right) + ns}{\left(t_r - t\right)^2} = m_1 x_3 + \dot{x}_3 + \frac{n\dot{s}\left(t_r - t\right) + ns}{\left(t_r - t\right)^2} \\ &= m_1 x_3 + f_0 + f_1 + bu + \frac{n\dot{s}\left(t_r - t\right) + ns}{\left(t_r - t\right)^2}, \end{aligned} \quad \ldots(57)$$

where $m_1 x_3 + f_0$ is known, and f_1 is a bounded uncertainty (which represents target manoeuvering). Therefore, from Theorem 2, the following guidance law:

$$u = -\frac{1}{b}\left(m_1 x_3 + f_0 + f_1 + \frac{n\dot{s}\left(t_r - t\right) + ns}{\left(t_r - t\right)^2} + \eta \mathrm{sgn}\left(\dot{s}_1 + \frac{ns}{t_r - t}\right)\right) \quad \ldots(58)$$

can make the system converge to zero in finite time, thereby guaranteeing accurate interception and impact angle constraint.

Notably, $f_1 = -\frac{2\dot{r}}{r}x_2 + \frac{1}{r}\dot{a}_{Tq}$ in guidance law Equation (58) is regarded as a system uncertainty, which makes the guidance law difficult to implement. Considering $\dot{r}$ exhibits minimal

https://doi.org/10.1017/aer.2020.28 Published online by Cambridge University Press

change, suppose $\dot{r} \approx \text{const}$; hence, $\ddot{r} \approx 0$, then $f_1 = -\frac{2\dot{r}}{r}x_2 + \frac{1}{r}\dot{a}_{Tq} \approx \frac{1}{r}\dot{a}_{Tq}$. Combining with Assumption 1 yields

$$\begin{aligned} |\dot{f}_1| &= \left|\frac{\ddot{a}_{Tq}r - \dot{a}_{Tq}\dot{r}}{r^2}\right| \\ &= \left|\frac{\ddot{a}_{Tq}}{r} - \frac{\dot{a}_{Tq}\left(v_T\cos\left(q-\theta_T\right) - v_M\cos\left(q-\theta_M\right)\right)}{r^2}\right|, \\ &\le \frac{A_2}{r_0} + \frac{A_1 v_T^{\max}}{r_0^2} + \frac{A_1 v_M^{\max}}{r_0^2} \\ &= L \end{aligned} \quad \ldots(59)$$

where $v_M^{\max}$ and $v_T^{\max}$ are the maximum velocities of the missile and the target, respectively; therefore, $\dot{f}_1$ is bounded.

The target manoeuvering related variable f_1 should be estimated to implement guidance law Equation (58). The following is an estimation of f_1:

Given Equation (57),

$$\dot{s}_2 = m_1 x_3 + f_0 + f_1 + bu + \frac{n\dot{s}\left(t_r - t\right) + ns}{\left(t_r - t\right)^2}. \quad \ldots(60)$$

The target manoeuvering estimator presented in Section 3.1 is used; thus,

$$\begin{cases} \dot{z}_0 = z_1 + k_1|s_2 - z_0|^{1-1/p}\text{sgn}\left(x - z_0\right) + m_1 x_3 + f_0 + bu + \frac{n\dot{s}(t_r-t)+ns}{(t_r-t)^2} \\ \dot{z}_1 = k_2|x - z_0|^{1-2/p}\text{sgn}\left(x - z_0\right) \end{cases} \quad \ldots(61)$$

From Theorem 1, the variable $z_0 \to s_2, z_1 \to f_1\left(x_2, \dot{a}_{Tq}\right)$ is in finite time.

Then, Equation (58) can be rewritten as

$$u = -\frac{1}{b}\left(m_1 x_3 + f_0 + z_1 + \frac{n\dot{s}\left(t_r - t\right) + ns}{\left(t_r - t\right)^2} + \eta\text{sgn}\left(\dot{s}_1 + \frac{ns}{t_r - t}\right)\right). \quad \ldots(62)$$

Precise interception with the expected impact angle can be achieved through command Equation (62).

Remark 5. The guidance law is derived analytically when considering autopilot lag, so the derivation process is complicated. However, the method is simple in practical application. Another method to design the guidance law considering autopilot lag is the dynamic surface control. The derivation process of this method is simple but its application is complex. Since the differential operation is replaced by the low-pass filter, there are still some calculation errors in this method.

5.0 SIMULATION AND ANALYSIS

The simulation results and analyses of the proposed NSO-SMGL are presented in this section, where a self-seeking interceptor missile is launched by an airplane to intercept a

https://doi.org/10.1017/aer.2020.28 Published online by Cambridge University Press

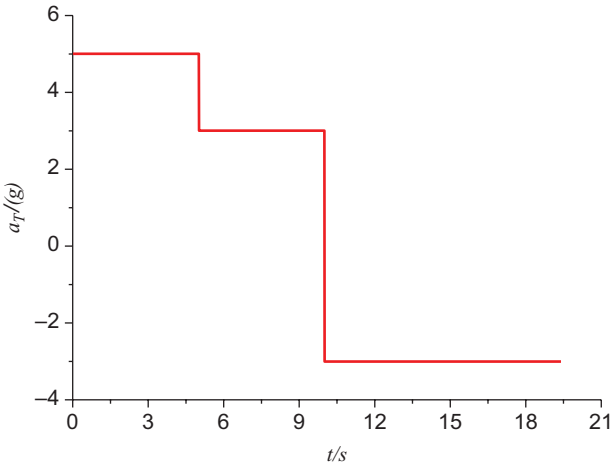

Figure 2. Target manoeuver form in Case 3.

manoeuvering target. In the simulation, the missile and the target move on the vertical plane. The initial position of the missile is $x_M(0) = 0\text{m}$, $y_M(0) = 1000\text{m}$. The initial position of the target is $x_T\ (0) = 4330\text{m}$, $y_T\ (0) = 3500\text{m}$. The flight speed of the missile is $v_M = 600\text{m/s}$, the initial flight path angle of the missile is $\theta_M\ (0) = 40°$, and the autopilot dynamic lag constant of the missile is $\tau = 0.5$. The initial speed of the target is $v_T\ (0) = 300\text{m/s}$, the initial flight path angle of the target is $\theta_T\ (0) = 0°$, and the initial LOS angle is $q_0 = 30°$. The simulation step size is 10ms, and the acceleration due to gravity $g = 9.8\text{m/s}^2$. To verify the effectiveness and superiority of NSO-SMGL, a target with different manoeuverings and a missile with different expected impact angles are divided into the following three cases.

Case 1: The target performs a step manoeuver, i.e. $a_T = 5\text{g}$. The expected LOS angle is $0° \leq q_d \leq 90°$ for every 30°.

Case 2: The target performs a periodic waving manoeuver, i.e., $a_T = 5g\sin(t)$. The expected LOS angle is $0° \leq q_d \leq 90°$ for every 30°.

Case 3: The target performs random step manoeuvers as shown in Fig. 2. The expected LOS angle is $0° \leq q_d \leq 90°$ for every 30°.

The target estimation parameters are $k_1 = 4$, $k_2 = 10$, and $p = 4.5$. NSO-SMGL with parameters $m_1 = 1$ and $n = 1.5$ is applied to the simulation.

The simulation results, including the trajectories of the missile and the target on the vertical plane, missile overload commands, sliding surface profiles, LOS angular velocity profiles, LOS angle profiles, and target manoeuvering estimations (uncertainty) are presented under different conditions in Figs. 3–5. NSO-SMGL can achieve high-precision interceptions to various types of manoeuvering targets within a wide range of expected impact angles as illustrated in the three figures. In Figs. 3(b)–5(b), the missile demands high control energy in the beginning of the terminal guidance phase because system states are far from the equilibrium. However, the overload commands are evidently reduced to a relatively lower level within an extremely short period. Such variation is beneficial for the guidance process, because the missile could produce high energy in the beginning of process and then gradually decrease

https://doi.org/10.1017/aer.2020.28 Published online by Cambridge University Press

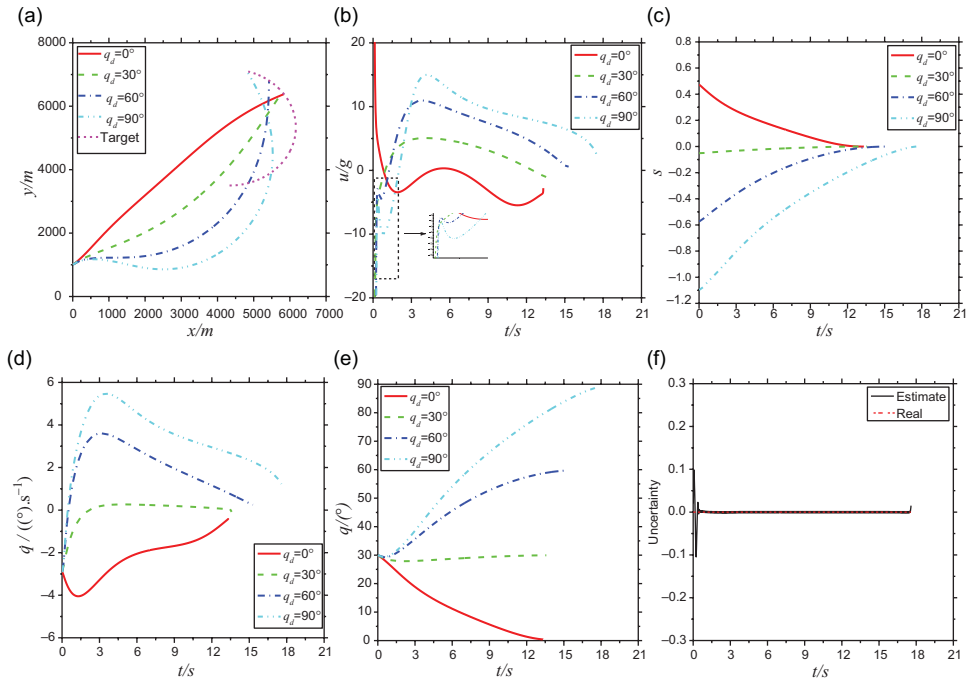

Figure 3. Simulation results of Case 1: (a) trajectories of missile and target, (b) missile overload commands, (c) sliding surface profiles, (d) LOS angular velocity, (e) LOS angle, and (f) target manoeuvering estimations.

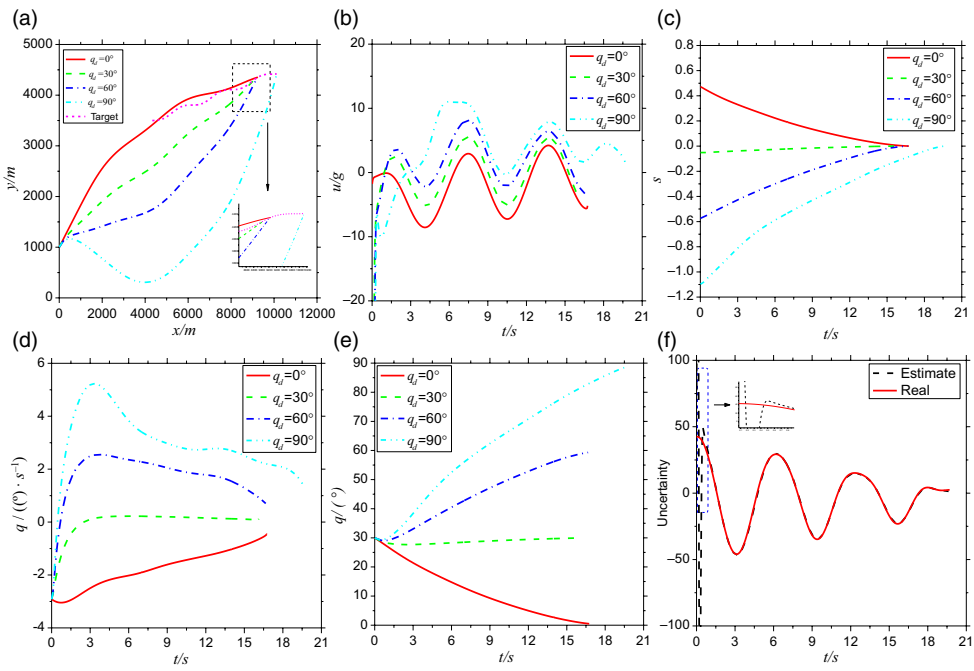

Figure 4. Simulation results of Case 2: (a) trajectories of missile and target, (b) missile overload commands, (c) sliding surface profiles, (d) LOS angular velocity, (e) LOS angle, and (f) target manoeuvering estimations.

https://doi.org/10.1017/aer.2020.28 Published online by Cambridge University Press

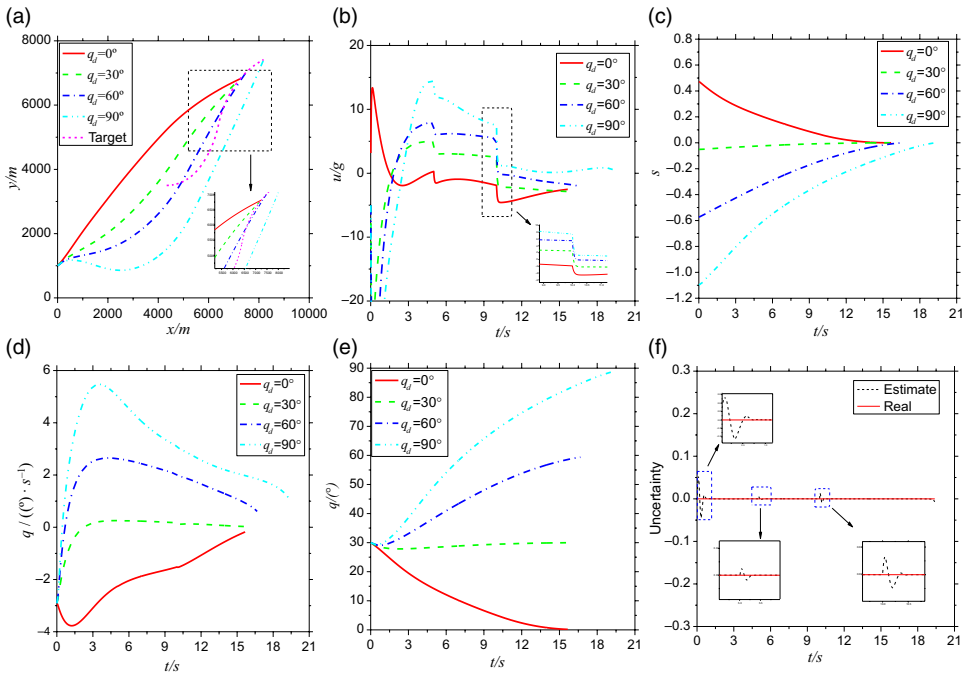

Figure 5. Simulation results of Case 3: (a) trajectories of missile and target, (b) missile overload commands, (c) sliding surface profiles, (d) LOS angular velocity, (e) LOS angle, and (f) target manoeuvering estimations.

during the flight. In Figs. 3(c)–5(c), the sliding surfaces gradually converge to zero, thereby avoiding oscillations between positive and negative values and preventing the unexpected chattering phenomenon. With the sliding surfaces converging to zero, the missile could hit the target at the desired angles. In Figs. 3(d), 3(e), 4(d), 4(e), 5(d), and 5(e), the LOS angular rate converges to zero and the LOS angle converges to expected values regardless of the target manoeuver, and the goal of the guidance law design is accomplished by considering autopilot lag. The estimation of uncertainty is $f_1 \approx (1/r)\dot{a}_{Tq}$ in theory, but uncertainty is minimal except at the end of the guidance process; therefore, the estimation results are multiplied by r. In Figs 3(f)–5(f), the performance of the target manoeuvering estimator achieves relatively satisfactory results. In the simulation, the missile could hit the manoeuvering target precisely, because the estimator obtains the target's acceleration effectively and compensates in guidance law. Even if there exists noises, the estimator can acquire the target's acceleration and noises together, and eliminate their influences in the final guidance law.

To further verify the efficiency of the proposed NSO-SMGL, the LSMGL proposed in[39], which considers the autopilot lag algorithm, is also used in the simulations for comparison. For the design of LSMGL, Equation (63) is selected as the sliding mode.

$$s = b_1 x_1 + b_2 x_2 + x_3. \qquad \ldots (63)$$

The definitions of x_1, x_2, and x_3 are the same as those in Section 4. The design parameters are b_1 and b_2.

https://doi.org/10.1017/aer.2020.28 Published online by Cambridge University Press

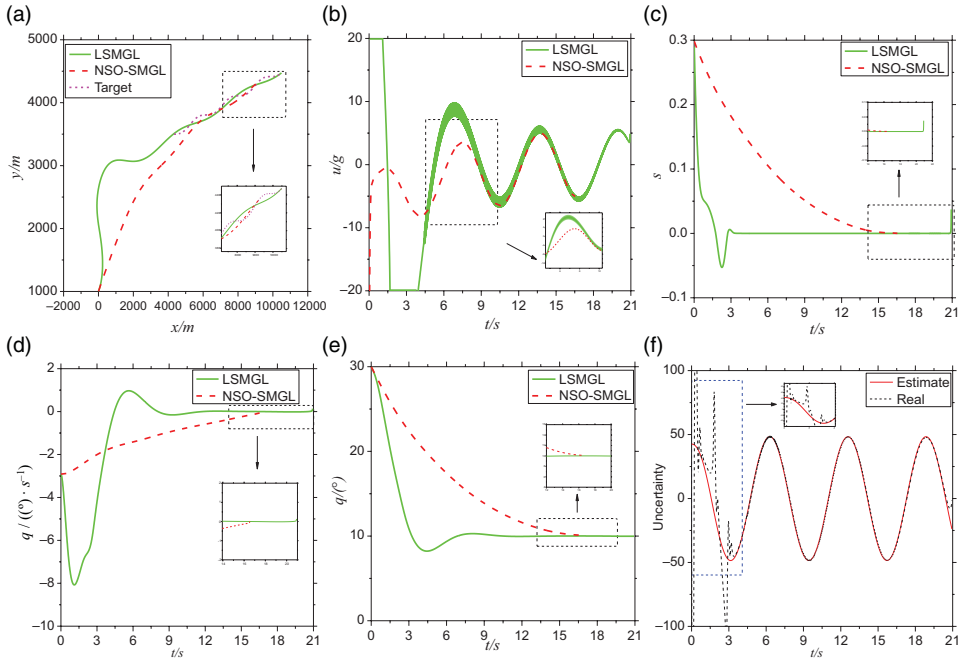

Figure 6. Comparison between LSMGL and NSO-SMGL: (a) trajectories of missile and target, (b) missile overload commands, (c) sliding surface profiles, (d) LOS angular velocity, (e) LOS angle, and (f) target manoeuvering estimations.

Differentiating Equation (63) yields

$$s = b_1 x_2 + b_2 x_3 + \dot{x}_3. \qquad \ldots (64)$$

The approach law is selected as follows:

$$\dot{s} = -ks - \sigma |s|^{\gamma} \operatorname{sgn}(s). \qquad \ldots (65)$$

LSMGL is deduced by substituting Equation (51) into Equation (64) and combining with Equation (65)

$$u = -\frac{1}{b}\left(b_1 x_2 + b_2 x_3 + f_0\left(x_3, a_{Mq}\right) + \ f_1\left(x_2, \dot{a}_{Tq}\right) + ks + \sigma |s|^{\gamma} \operatorname{sgn}(s)\right), \qquad \ldots (66)$$

where $f_0\left(x_3, a_{Mq}\right)$ and $f_1\left(x_2, \dot{a}_{Tq}\right)$ are the same as those in Section 3. Let $\hat{f}_1\left(x_2, \dot{a}_{Tq}\right)$ be an estimation of $f_1\left(x_2, \dot{a}_{Tq}\right)$. Then, guidance can be rewritten as

$$u = -\frac{1}{b}\left(b_1 x_2 + b_2 x_3 + f_0\left(x_3, a_{Mq}\right) + \hat{f}_1\left(x_2, \dot{a}_{Tq}\right) + ks + \sigma |s|^{\gamma} \operatorname{sgn}(s)\right), \qquad \ldots (67)$$

where $b_1 = 1$, $b_2 = 1$, $k = 1$, $\sigma = 1$, and $\gamma = 0.5$. The simulation with terminal condition $q_d = 0°$ cannot be accomplished via guidance law Equation (67); therefore, the terminal condition is modified to $q_d = 10°$. Other conditions are the same as those in Case 2. Figure 6

https://doi.org/10.1017/aer.2020.28 Published online by Cambridge University Press

presents the simulation results. Both methods enable the LOS angle to approach the desired value and the LOS angular velocity to approach zero. However, the sliding surface of LSMGL rapidly converges to zero and oscillate between positive and negative values, thereby making the overload in the beginning of the guidance process immense and trajectory bending evident. The high-frequency chattering phenomenon occurs in LSMGL guidance law. The results illustrate the drawbacks of the first-order sliding mode. The trajectory of NSO-SMGL is smooth, and the guidance law exhibits no chattering, because the sliding surface has a relative degree of 2 and the observer is finite-time convergence and exhibits strong robustness against the variation of target manoeuverings. The simulation results verify the validity of the theory in Section 3.2, i.e., the advantage of the proposed NSO-SMGL is ensuring that the sliding surface and its derivative converge to zero in finite time and guaranteeing that the sliding surface does not cross zero until the ultimate time. Moreover, the proposed guidance law achieves a wider range of intercept angles than LSMGL. In summary, the performance of the proposed NSO-SMGL Equation (62) is superior to that of the general LSMGL Equation (67) and the associated drawbacks of LSMGL are overcome.

6.0 CONCLUSIONS

This study presents NSO-SMGL for intercepting manoeuvering targets by considering autopilot lag and terminal impact angle constraint. The proposed NSO-SMGL is constructed by combining a target manoeuvering estimator and a novel smooth second-order sliding mode through the application of a backstepping technique. The guidance law ensures that the sliding surface and its derivative converge to zero in finite time while guaranteeing that the sliding surface will not cross zero until the ultimate time, thereby effectively eliminating undesired chattering. Depending on the advantages of the target estimator, the presented NSO-SMGL requires no information regarding the target and provides a relatively effective estimation of the target manoeuvering, thereby making its implementation possible. The convergence of the guidance system is proven on the basis of Lyapunov stability theory. The simulation results of the comparisons with LSMGL validate the effectiveness and superiority of the proposed guidance system. Our future research will concentrate on the actuators saturation, dynamic characteristics of higher order autopilots and the guidance law in three-dimensional plane.

REFERENCES

1. KIM, M. and GRIDER, K.V. Terminal guidance for impact attitude angle constrained flight trajectories. *IEEE Transactions on Aerospace and Electronic Systems*, 1973, **9**, (6), pp 852–859.
2. BRYSON, A.E. Jr. AND HO, Y.C. *Applied Optimal Control*, Wiley, 1975, New York, NY, US.
3. CHO, H. Navigation constants in PNG law and the associated optimal control problems (in Korean), In Proceedings of Korean Automatic Control Conference, Seoul, Korea, Oct. 1992, pp 578–583.
4. RYOO, C.K., CHO, H. and TAHK, M.J. Optimal guidance laws with terminal impact angle constraint. *J Guidance, Control, and Dynamics*, 2005, **28**, (4), pp 724–732.
5. RATNOO, A. and GHOSE, D. State-dependent Riccati-equation-based guidance law for impact angle constrained trajectories. *J Guidance, Control, and Dynamics*, 2009, **32**, (1), pp 320–325.
6. LEE, Y.I., KIM, S.H. and TAHK, M.J. Optimality of linear time-varying guidance for impact angle control. *IEEE Transactions on Aerospace and Electronic Systems*, 2012, **48**, (3), pp 2802–2817.
7. MAITY, A., OZA, H.B. and PADHI, R. Generalized model predictive static programming and angle-constrained guidance of air-to-ground missiles, *J Guidance, Control, and Dynamics*, 2014, **37**, (6), pp 1897–1913.

https://doi.org/10.1017/aer.2020.28 Published online by Cambridge University Press

8. OZA, H.B. and PADHI, R. Impact angle constrained suboptimal model predictive static programming guidance of air-to-ground missiles, *J Guidance, Control, and Dynamics*, 2012, **35**, (1) pp 153–164.
9. KIM, B.S., LEE, J.G. and HAN, H.S. Biased PNG law for impact with angular constraint. *IEEE Transactions on Aerospace and Electric Systems*, 1998, **34**, (1), pp 277–288.
10. RATNOO, A. and GHOSE, D. Impact angle constrained interception of stationary targets. *J Guidance, Control, and Dynamics*, 2008, **31**, (6), pp 1816–1821.
11. RATNOO, A. and GHOSE, D. Impact angle constrained guidance against nonstationary nonmaneuvering targets. *J Guidance, Control, and Dynamics*, 2010, **32**, (1), pp 269–275.
12. ERER, K.S. and MERTTOPÇUOĞLU, O. Indirect impact-angle-control against stationary targets using biased pure proportional navigation. *J Guidance, Control, and Dynamics*, 2012, **35**, (2), pp 700–703.
13. LI, T., ZHAO R. and CHEN C.L.P, et al. Finite-time formation control of under-actuated ships using nonlinear sliding mode control. *IEEE Transactions on Cybernetics*, 2018, **48**, (11), pp 3243–3253.
14. DEYIN, Y., BIN, Z. and PANSHUO, L, et al. Event-triggered sliding mode control of discrete-time Markov jump systems. *IEEE Transactions on Systems, Man, and Cybernetics: Systems*, 2019, **49**, (10), pp 2016–2025.
15. LEE, C.H., KIM, T.H. and TAHK, M.J. Design of impact angle control guidance laws via high-performance sliding mode control, *Proceedings of the Institution of Mech Engineers, Part G: J Aerospace Engineering*, 2013, **227**, (2), pp 235–253.
16. RAO, S. and GHOSE, D. Sliding mode control based terminal impact angle constrained guidance laws using dual sliding surfaces, Proceedings of 12th IEEE Workshop on Variable Structure Systems, IEEE Publ., Piscataway, NJ, 2012, pp 325–330.
17. HE, S.M. and LIN, D.F. A robust impact angle constraint guidance law with seeker's field-of-view limit, *Transaction of the Institute of Measurement and Control*, 2014, **37**, (3), 317–328.
18. KUMAR, S.R., RAO, S. and GHOSE, D. Sliding-mode guidance and control for all-aspect interceptors with terminal angle constraints, *J Guidance, Control, and Dynamics.* 2012, **35**, (4), pp 1230–1246.
19. KUMAR, S.R., RAO, S. and GHOSE, D. Nonsingular terminal sliding mode guidance with impact angle constraints, *J Guidance, Control, and Dynamics*, 2014, **37**, (4), pp 1114–1130.
20. HE, S.M., LIN, D.F. and WANG, J. Continuous second-order sliding mode based impact angle guidance law, *Aerospace Science and Technology*, 2015, **41**, pp 199–208.
21. SUN, S., ZHOU, D. AND HOU, W. A guidance law with finite time convergence accounting for autopilot lag, *Aerospace Science and Technology*, 2013, **25**, (1), pp 132–137.
22. ZHANG, T., GE, S.S. and HANG, C.C. Adaptive neural network control for strict-feedback nonlinear systems using backstepping design, *Automatica*, 2000, **36**, pp 1835–1846.
23. CHOI, J.Y. and FARRELL, J.A. Adaptive observer backstepping control using neural networks, *IEEE Transactions on Neural Networks*, 2001, **12**, (5), pp.1103–1112.
24. KULJACA, O., SWAMY, N. and LEWIS, F. L., et al. Design and implementation of industrial neural network controller using backstepping, Proceedings of the 40th IEEE Conference on Decision and Control, IEEE, 2001.
25. LIN, C.M. and HSU, C.F. Recurrent-neural-network-based adaptive backstepping control for induction servomotor, *IEEE Transactions on Industrial Electronics*, 2005, **52**, (6), pp 1677–1684.
26. HSU, C.F., LIN, C.M. and LEE, T.T. Wavelet adaptive backstepping control for a class of nonlinear systems. *IEEE Transactions on neural networks*, 2006, **17**, (5), 1175–1183.
27. ZHAO, X., YANG, H. and KARIMI, H.R., et al. Adaptive neural control of MIMO nonstrict-feedback nonlinear systems with time delay. *IEEE Transactions on Cybernetics*, 2015, **46**, (6), 1337–1349.
28. TONG, S., LI, Y. and SHI, P. Observer-based adaptive fuzzy backstepping output feedback control of uncertain MIMO pure-feedback nonlinear systems, *IEEE Transactions on Fuzzy Systems*, 2012, **20**, (4), pp 771–785.
29. WANG, T., ZHANG, Y. and QIU, J., et al. Adaptive fuzzy backstepping control for a class of nonlinear systems with sampled and delayed measurements, *IEEE Transactions on Fuzzy Systems*, 2015, **23**, (2), pp. 302–312.
30. DU, H. and CHEN, X. NN-based output feedback adaptive variable structure control for a class of non-affine nonlinear systems: a nonseparation principle design, *Neuro Computing*, 2009, **72**, pp 2009–2016.

https://doi.org/10.1017/aer.2020.28 Published online by Cambridge University Press

31. AREFI, M.M., ZAREI, J. and KARIMI H.R. Adaptive output feedback neural network control of uncertain non-affine systems with unknown control direction, *J Franklin Institute*, 2014, **351**, (8), 4302–4316.
32. DONG, X., ZHAO, Y. and KARIMI, H.R., et al. Adaptive variable structure fuzzy neural identification and control for a class of MIMO nonlinear system, *J Franklin Institute*, 2013, **350**, pp 1221–1247.
33. ZHANG Y., TANG S.J. and GUO, J. An adaptive fast fixed-time guidance law with an impact angle constraint for intercepting maneuvering targets. *Chinese J Aeronautics*, 2018, **147**, (6), pp 167–184.
34. BHAT, S.P. and BERNSTEIN, D.S. Continuous finite-time stabilization of the translational and rotational double integrators, IEEE Int Conference on Control Applications, 2002.
35. BHAT, S.P. and BERNSTEIN, D.S. Finite-time stability of continuous autonomous systems, *Soc for Industrial and Applied Mathematics*, 2000, **38**, (3), pp 751–766.
36. HE, S.M. and LIN D.F. Guidance laws based on model predictive control and target maneuver estimator, *Transactions of the Institute of Measurement and Control*, 2016, **38**, (12), pp 1509–1519.
37. LEVANT, A. Construction principles of 2-Sliding mode design, *Automatica*, 2007, **43**, (4), pp 576–586.
38. NATHAN, H. and BALAKRISHNAN, S.N. Impact Time and Angle Guidance with Sliding Mode Control, *IEEE Transactions on control systems technology*, 2012, **20**, (6), pp 1436–1449.
39. ZHOU, H.B. *Study on Guidance Law and Cooperative Guidance for Multi-Missiles Based on Finite-Time and Sliding Mode Theory*, Harbin Institute of Technology, 2015, Harbin, China, pp 63–66.

https://doi.org/10.1017/aer.2020.28 Published online by Cambridge University Press